**US-FT/5-96**
**hep-ph/9602230**

# FAST ANTIBARYON PRODUCTION IN $pp$ COLLISIONS AS A RESULT OF STRING FUSION

arXiv:hep-ph/9602230v1 6 Feb 1996

N. Armesto, E. G. Ferreiro, C. Pajares and Yu. M. Shabelski*

*Departamento de Física de Partículas, Universidade de Santiago de Compostela, 15706-Santiago de Compostela, Spain*

**ABSTRACT**

The inclusion of string fusion in Dual Parton Model results in the appearance of diquark-antidiquark pairs in the sea with comparatively large Feynman-$x$. Such antidiquarks can fragment into fast antibaryons, thus increasing several times the corresponding yields in high energy $pp$ collisions for $x_F \sim 0.8 \div 0.9$. String fusion also results in an unusual dependence of inclusive spectra on the multiplicity of secondaries. Some numerical estimations are presented.

*Permanent address: Leningrad Nuclear Physics Institute, Gatchina, Sanct-Petersburg 188350, USSR.

**US-FT/5-96**
**February 1996**

## 1. INTRODUCTION

Models based on pomeron exchange are very popular for the description of multiparticle production on nucleon and nuclear targets at high energies (see for example [1, 2]). In the simplest approach pomerons are assumed not to interact one with each other. In this case the relative content of secondaries produced in nucleon-nucleon, nucleon-nucleus and nucleus-nucleus collisions should be practically the same because all secondaries are produced inside a pomeron (in the sense of the unitarity condition)[1]. Only very small differences are possible because when a different number of pomerons are cut, secondaries are produced at different effective energies.

However in high energy heavy ion collisions a relative enhancement of strange secondary production in comparison with *pp* collisions has been experimentally found [3]. The most natural way to explain such effects in the framework of pomeron-based models seems to be assuming that pomeron interactions are more essential in the case of nucleus-nucleus collisions than in the case of *pp* interactions [4] (simply because of larger combinatorial factors). We discuss below that in the case of the cut of a diagram with interacting pomerons colour strings should connect not only valence quarks and diquarks and sea quarks, but also with sea diquarks and antidiquarks (coming from the fusion of two quark-antiquark strings). These latter fragment preferably into baryons and antibaryons so their appearance can change the content of secondaries (making possible to explain the strangeness and antibaryon enhancement, [5]).

String fusion should exist with a small probability in the case of high energy *pp* collisions and result in antibaryon production with very high Feynman-$x$. Model estimations predict a yield of such antibaryons several times larger than in the case of a variant without string fusion. On the other hand the case of *pp* collisions looks more clean in comparison with interactions on nuclear targets. So the appearance of such fast antibaryons can be considered as an evidence for the existence of this kind of collective effects. For numerical estimations in Section 3 we use the Quark-Gluon String Model (QGSM) [1] which describes quite successfully the spectra of different secondaries produced in high energy hadron-nucleon and hadron-nucleus collisions, see for example [1, 6]. This model is very close to the Dual Parton Model [2]. In particular the spectrum of $\Lambda_s$, to which the fragmentation of a valence diquark gives the main contribution[2] at large $x_F$, is described well enough so we can hope that the parameters of antibaryon production by sea-antidiquark fragmentation are more or less fixed.

String fusion also changes the dependence of inclusive spectra on the multiplicity. Usually the spectrum of any particle for events with multiplicity higher than the mean one becomes more and more narrow, due to the division of the initial energy between

[1] Each cut pomeron gives rise to two colour strings streched between partons of the projectile and target; the strings decay afterwards into the observed secondaries.

[2] In the case of high $x_F$ proton production in *pp* collisions triple-reggeon diagrams give the main contribution.

many cut pomerons. However for a particle whose spectrum in the large $x_F$ region is determined by string fusion the behaviour becomes the opposite, i.e., the spectrum gets constant or even broader.

## 2. INCLUSIVE SPECTRA OF SECONDARY HADRONS IN QGSM

In the QGSM high energy hadron-nucleon and hadron-nucleus interactions are considered as proceeding via the exchange of one or several pomerons. Each pomeron corresponds to a cylindrical diagram, so in the case of one cut pomeron two showers of secondaries are produced, see Fig. 1. The inclusive spectrum of secondaries is determined by the convolution of the diquark and valence and sea quark distributions $u(x,n)$ in the incident particles with the fragmentation functions of quarks and diquarks into secondary hadrons $G(z)$. The diquark and quark distribution functions depend on the number $n$ of cut pomerons in the considered diagram. For a nucleon target the inclusive spectrum of a secondary hadron $h$ has the form [1]

$$\frac{x_E}{\sigma_{inel}}\,\frac{d\sigma}{dx_F} = \sum_{n=1}^{\infty} w_n \phi_n^h(x)\ , \tag{1}$$

where the function $\phi_n^h(x)$ determines the contribution of the diagram with $n$ cut pomerons and $w_n$ is the probability of this diagram. We neglect diffractive dissociation, as its effect is known to be comparatively small in the case of antibaryon production.

For $pp$ collisions:

$$\phi_n^h(x) = f_{qq}^h(x_+,n) f_q^h(x_-,n) + f_q^h(x_+,n) f_{qq}^h(x_-,n) + 2(n-1) f_s^h(x_+,n) f_s^h(x_-,n)\ , \tag{2}$$

$$x_\pm = \frac{1}{2}[\sqrt{4m_T^2/s + x^2} \pm x]\ , \tag{3}$$

where $f_{qq}$, $f_q$ and $f_s$ correspond to the contribution to the inclusive spectrum of diquarks, valence and sea quarks respectively. They are determined by the convolution of diquark and quark distributions with fragmentation functions,

$$f_q^h(x_+,n) = \int_{x_+}^1 u_q(x_1,n) G_q^h(x_+/x_1)\, dx_1\ . \tag{4}$$

Both diquark and quark distributions and fragmentation functions are expressed via their Regge-asymptotics, taking into account the conservation laws [1, 7].

In the calculations we use quark and diquark distributions in the proton of the form [1]:

$$u_{uu}(x,n) = C_{uu}\, x^{2.5}(1-x)^{n-1.5}\ , \tag{5}$$

$$u_{ud}(x,n) = C_{ud}\, x^{1.5}(1-x)^{n-1.5}\ , \tag{6}$$

$$u_u(x,n) = C_u\ x^{-0.5}(1-x)^{n+0.5}\ , \tag{7}$$

$$u_d(x,n) = C_d\ x^{-0.5}(1-x)^{n+1.5}\ , \tag{8}$$

$$u_{\overline{u}}(x,n) = u_{\overline{d}}(x,n) = C_{\overline{u}}\ x^{-0.5}[(1+\delta/2)(1-x)^{n+0.5}(1-x/3)-\delta\ (1-x)^{n+1}/2]\ ,\ n>1\ , \tag{9}$$

$$u_s(x,n) = C_s\ x^{-0.5}(1-x)^{n+1}\ ,\ n>1\ . \tag{10}$$

$\delta = 0.2$ is the relative probability to find a strange quark in the sea and the factors $C_i$ are determined from the normalization condition

$$\int_0^1 u_i(x,n)dx = 1\ . \tag{11}$$

Quark and diquark fragmentation functions into secondary hadrons are taken from [1, 7].

In the case of baryon $B$ production in $pp$ collisions there are two different contributions [8]. The first one corresponds to the central production of a $B\overline{B}$ pair and can be described by the formulas written above. The second contribution is connected with the direct fragmentation of the initial proton into $B$ with conservation of the string junction. To account for this possibility we input into Eq. (2) two additional items $f_{qq2}(x_+,n)$ for $x_F > 0$ and $f_{qq2}(x_-,n)$ for $x_F < 0$ which are not multiplied by $f_q(x_-,n)$ and $f_q(x_+,n)$ respectively. The form of $f_{qq2}(x_+,n)$ and $f_{qq2}(x_-,n)$ is determined by the corresponding fragmentation functions. For example, in the case of $\Lambda_s$ production they are

$$G^{\Lambda_c}_{uu2} = a_{02}\ z^2(1-z)^{1+\lambda-\alpha_\varphi(0)} \tag{12}$$

and

$$G^{\Lambda_c}_{ud2} = a_{02}\ z^2(1-z)^{\lambda-\alpha_\varphi(0)}\ , \tag{13}$$

with $\lambda = 0.5$ and $\alpha_\varphi(0) = 0$.

The probability of a process with $n$ cut pomerons is calculated in the quasieikonal approximation [1, 9]:

$$w_n = \sigma_n/\sum_{n=1}^{\infty}\sigma_n\ ,\ \sigma_n = \frac{\sigma_P}{nz}(1-e^{-z}\sum_{k=0}^{n-1}\frac{z^k}{k!})\ , \tag{14}$$

$$z = \frac{2\ C\ \gamma}{R^2+\alpha'\xi}e^{\Delta\xi}\ ,\ \sigma_P = 8\pi\gamma e^{\Delta\xi}\ ,\ \xi = \ln(s/1\ GeV^2)\ , \tag{15}$$

with

$$\Delta = 0.139\ ,\ \alpha' = 0.21\ GeV^{-2}\ ,\ \gamma_{pp} = 1.77\ ,\ \gamma_{\pi p} = 1.07\ ,$$

$$R^2_{pp} = 3.18\ GeV^{-2}\ ,\ R^2_{\pi p} = 2.48\ GeV^{-2}\ ,\ C_{pp} = 1.5\ ,\ C_{\pi p} = 1.65\ .$$

## 3. STRING FUSION CONTRIBUTION IN QGSM

A possible mechanism of string fusion can be inferred if we consider the intermediate states of a triple-reggeon diagram. Let us consider such a diagram in which a triple-reggeon exchange connects sea quarks of two interacting nucleons and let all reggeons be cut, Fig. 2a[3]. One possible inelastic intermediate state is shown in Fig. 2b (we present only one of the two produced chains, compare to Fig. 1c). If in the upper part of the diagrams in Fig. 2 two pomerons are connected with two sea quarks, in the lower part a reggeon will interact with two sea antiquarks because every chain as a whole has to be white. So the ends of the strings (two antiquarks in this case) can fuse and produce some new object which will fragment into secondary hadrons as a whole. We will call this object a sea antidiquark.

In the QGSM an incident fast quark is assumed to fragment into a hadron (say, a meson) producing a slower quark which will fragment again and so on, until it fuses with a target diquark or antiquark, forming respectively a baryon or a meson. In the case shown in the Fig. 2b the same process will occur in the upper part. However a sea diquark will appear at a rapidity value approximately equal to the rapidity of the triple-reggeon vertex. Then two possibilities appear: it can fragment into a baryon $B$ as shown in Fig. 2b or into mesons until its annihilation with the sea antidiquark. It is in the first possibility that we can obtain a comparatively fast antibaryon in the backward hemisphere. Let us note that the lower reggeon in Fig. 2a corresponds to the pomeron at high energies. This is clear if we compare the sea diquark-antidiquark interaction in Fig. 2b to the valence diquark-antidiquark interaction in the case of high energy $p\overline{p}$ interactions.

The process of fusion of two sea quarks (antiquarks) into one sea diquark (antidiquark) becomes possible for $n \geq 3$ in Eq. (1). It seems that the best place to see the effects of string fusion is in the spectra of fast antibaryons produced in $pp$ collisions because the contribution of all other processes is comparatively small. The enhancement of these spectra in the large $x_F$ region in the case of string fusion arises from two facts: i) the $x$-distribution of sea antidiquarks is harder than that of sea antiquarks and ii) the fragmentation functions are harder.

For the numerical estimations which are, of course, model dependent, we take the probability of two sea quarks fusing into a diquark equal to $v_0 = 0.02$. So the probability to find two fused quarks in a diagram with a $n$-pomeron exchange is:

$$v_n = v_0 \, (n-1) \, (2n-3) \tag{16}$$

(the probability that these quarks are both antiquarks is separately accounted for). As a result, the total probability for string fusion in inelastic $pp$ collisions is

$$w_{fus} = \sum_{n=3}^{\infty} v_n \, w_n \ , \tag{17}$$

[3]Other reggeons which connect valence quarks are not shown for simplicity.

which is about 1/20 at $\sqrt{s} = 39$ GeV. This is close to the standard contribution of triple-reggeon diagrams at this energy.

For the $x$-distributions of sea antidiquarks we use the simplest assumption: it is a convolution of two sea quark distributions,

$$u_{\overline{qq}}(x,n) = \int u_{\overline{q}}(x_1,n) u_{\overline{q}}(x_2,n)\ \delta(x - x_1 - x_2)\ dx_1 dx_2 \tag{18}$$

and we use the standard functions [1, 7] for their fragmentation into antibaryons.

The results for the $x_F$-spectra of $\overline{p}$ and $\overline{\Lambda}_s$ produced in $pp$ collisions at different energies are shown in Figs. 3 and 4. Model predictions without string fusion are shown by solid lines and with string fusion by dashed lines. In all cases the difference in the small $x_F$ region is very small and decreasing with energy. The reason is that sea antidiquarks have an average $x_F$ value not so small – about $0.1 \div 0.15$, so they are far (in rapidity) from the central region. In the large $x_F$ region the difference becomes larger and it is about one order of magnitude at $x_F = 0.85 \div 0.9$ (almost independently on the initial energy).

## 4. THE SHAPE OF INCLUSIVE SPECTRA IN EVENTS WITH DIFFERENT MULTIPLICITY

Let us take a sample of multiparticle production data without low multiplicity events, say with $n_{ch} \geq < n_{ch} >$. Usually the spectra of secondaries in such a sample become more narrow than that for standard events. The reason is that events corresponding to one-pomeron cut have on the average a smaller multiplicity of secondaries in comparison with multipomeron events, so one-pomeron events are more frecuently suppressed from our high multiplicity sample. Then such a sample is rich in multipomeron events. But it is in these events where the $x$-distributions of quarks and diquarks (ends of strings), Eqs. (5)-(10), are more narrow (simply because the energy has to be divided between more partons), so these quarks and diquarks will generate a more narrow spectrum of secondaries.

However if string fusion is taken into account the behaviour of the spectrum is more complicated. For secondary mesons or baryons produced in $pp$ collisions we can only expect some small quantitative difference because the string fusion contribution is small practically at all $x_F$. But in the case of the antibaryon spectrum string fusion dominates the region of large $x_F$ (Figs. 3 and 4). After substracting the low multiplicity events the inclusive cross section in this region will change only slightly[4]. On the other hand it will decrease more or less significantly in the small $x_F$ region where one-pomeron processes give about one half of the inclusive cross section. So we can expect that the spectrum of antibaryons becomes even wider in the set of high multiplicity events.

[4]The $x$-distribution of sea antidiquarks is wider than those of sea antiquarks, as it results from adding the $x$'s of the two parent sea antiquarks, Eq. (18).

For numerical estimations let us define the variable

$$z = \frac{n_{ch}}{< n_{ch} >} \tag{19}$$

and consider the spectra of secondary antibaryons for events with $z \geq z_0$. $z_0 = 0$ means that we take all events (minimal bias sample), for $z_0 = 1$ we take only events with multiplicity of charged secondaries larger than the mean one and so on.

As the differences in the shapes of the are not very large it is better to consider the ratio of the inclusive cross section in two different points, $x_1$ and $x_2$,

$$R\Big(\frac{x_F = x_1}{x_F = x_2}\Big) = \frac{[x_E/\sigma_{inel} \;\; d\sigma/dx_F]|_{x_F=x_1}}{[x_E/\sigma_{inel} \;\; d\sigma/dx_F]|_{x_F=x_2}} \;, \tag{20}$$

as a function of $z_0$.

The model estimations of these ratios for $x_1 = 0.6$ (where the cross section is not very small) and $x_2 = 0$ are presented in Fig. 5 for $\overline{p}$ and $\overline{\Lambda}_s$ produced in $pp$ collisions at energy $\sqrt{s} = 39$ GeV. It can be seen that in both cases there exists a large difference in the behaviour of the ratios without (solid curves) and with (dashed curves) string fusion. The experimental investigation of such ratios could give evidence on the existence of string fusion.

## 5. CONCLUSIONS

The existence of triple-reggeon interaction has been firmly confirmed by experiment. The string fusion mechanism is a simple possibility to incorporate the contribution of such diagrams into a model of multiparticle production. The difference in the content of secondaries between high energy nucleon-nucleon and nucleus-nucleus collisions can be explained if one takes into accountthe contribution coming from string fusion. However some numerically small effect should also exists in the case of high energy $pp$ (or $\overline{p}p$) interactions. It can be observed as an enhancement of secondary antibaryon production and an unusual dependence of the shapes of their inclusive spectra on the multiplicity of secondaries.

We thank the Dirección General de Política Científica and the CICYT of Spain for financial support. E.G.F also thanks the Xunta de Galicia for for financial support The paper was supported in part by INTAS grant 93-0079.

# References


[1] A.B.Kaidalov and K.A.Ter-Martirosyan. Yad.Fiz. 39 (1984) 1545; 40 (1984) 211.

[2] A.Capella, U.P.Sukhatme, C.-I.Tan and J.Tran Thanh Van. Phys.Rep. 236 (1994) 225.
K.Werner. Phys.Rep. 232 (1993) 87.

[3] NA35 Collaboration, presented by D.Röhrich and M.Gazdzicki at the QM'93 Conference, Frankfurt preprints IFK-HENGPG/93-8 (1993), 94-1 (1994) and 93-6 (1993).
E.Andersen et al. Phys.Lett. B316 (1993) 603.
S.Abatzis et al. Phys.Lett. B270 (1991) 123.

[4] M.A.Braun and C.Pajares. Phys.Lett. B287 (1992) 154; Nucl.Phys. B390 (1993) 542; 559.

[5] N.S.Amelin, M.A.Braun and C.Pajares. Phys.Lett. B306 (1993) 312; Z. Phys. C-Particles and Fields 63 (1994) 507.
N.Armesto, M.A.Braun, E.G.Ferreiro and C.Pajares. Phys.Lett. B344 (1995) 301.
H.Sorge, M.Berenguer, H.Stöcker and W.Greiner. Phys.Lett. B289 (1992) 6.

[6] Yu.M.Shabelski. Z.Phys. C-Particles and Fields 38 (1988) 569.

[7] Yu.M.Shabelski. Yad.Fiz. 44 (1986) 186.

[8] A.B.Kaidalov and O.I.Piskunova. Yad.Fiz. 43 (1986) 1545; Z. Phys. C-Particles and Fields 30 (1986) 145.

[9] K.A.Ter-Martirosyan. Phys.Lett. 44B (1973) 377.

## Figure captions

**Fig. 1.** Cylindrical diagram which corresponds to the one-pomeron exchange contribution to elastic $pp$ scattering (a). Its cut which determines the contribution to inelastic $pp$ cross section (b). The diagram which corresponds to the cut of three pomerons (c).

**Fig. 2.** Cut triple-reggeon diagram (a) and the corresponding inelastic intermediate state (b) with baryon-antibaryon production via string fusion.

**Fig. 3.** The predicted inclusive spectra of antiprotons in $pp$ collisions at $\sqrt{s} = 39$ (a), 200 (b) and 1800 (c) GeV without (solid curves) and with (dashed curves) string fusion.

**Fig. 4.** The predicted inclusive spectra of $\overline{\Lambda}_s$ in $pp$ collisions at $\sqrt{s} = 39$ (a), 200 (b) and 1800 (c) GeV without (solid curves) and with (dashed curves) string fusion.

**Fig. 5.** The predicted ratios of $\overline{p}$ (a) and $\overline{\Lambda}_s$ (b) inclusive spectra in $pp$ collisions at $\sqrt{s} = 39$ GeV without (solid curves) and with (dashed curves) string fusion.

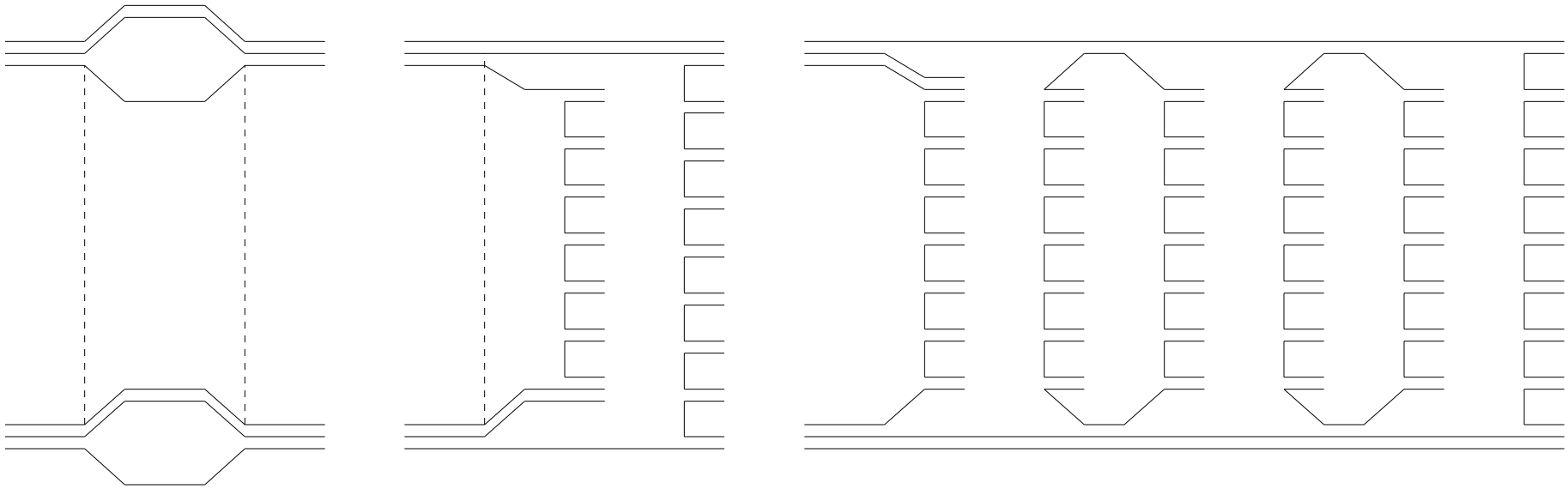



Fig. 1

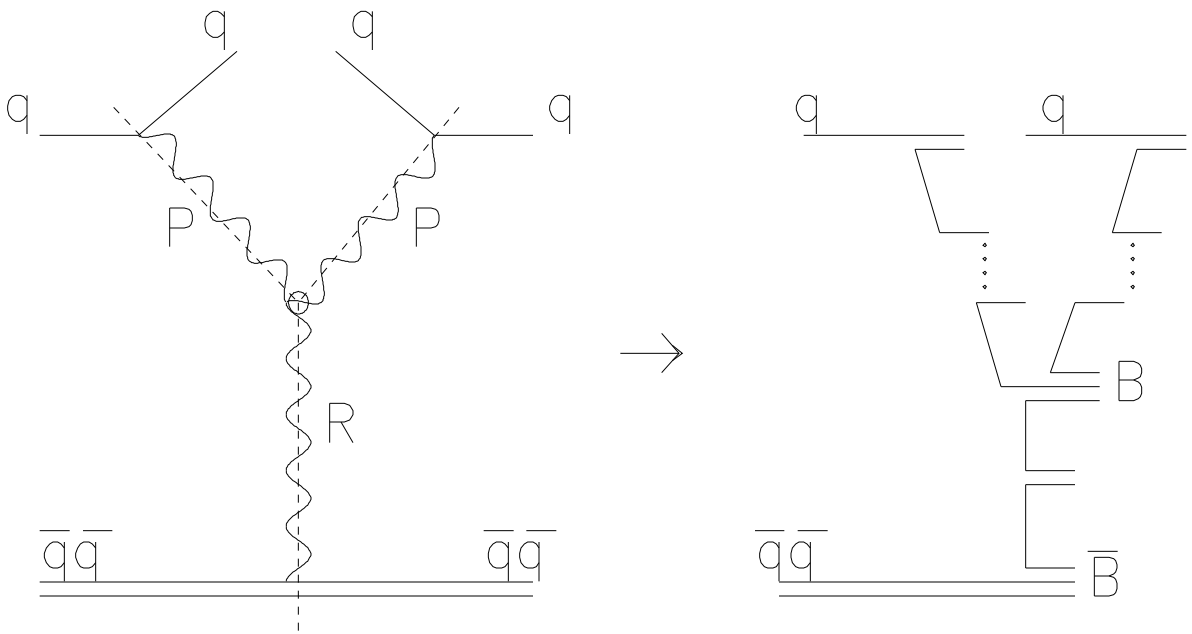



Fig. 2

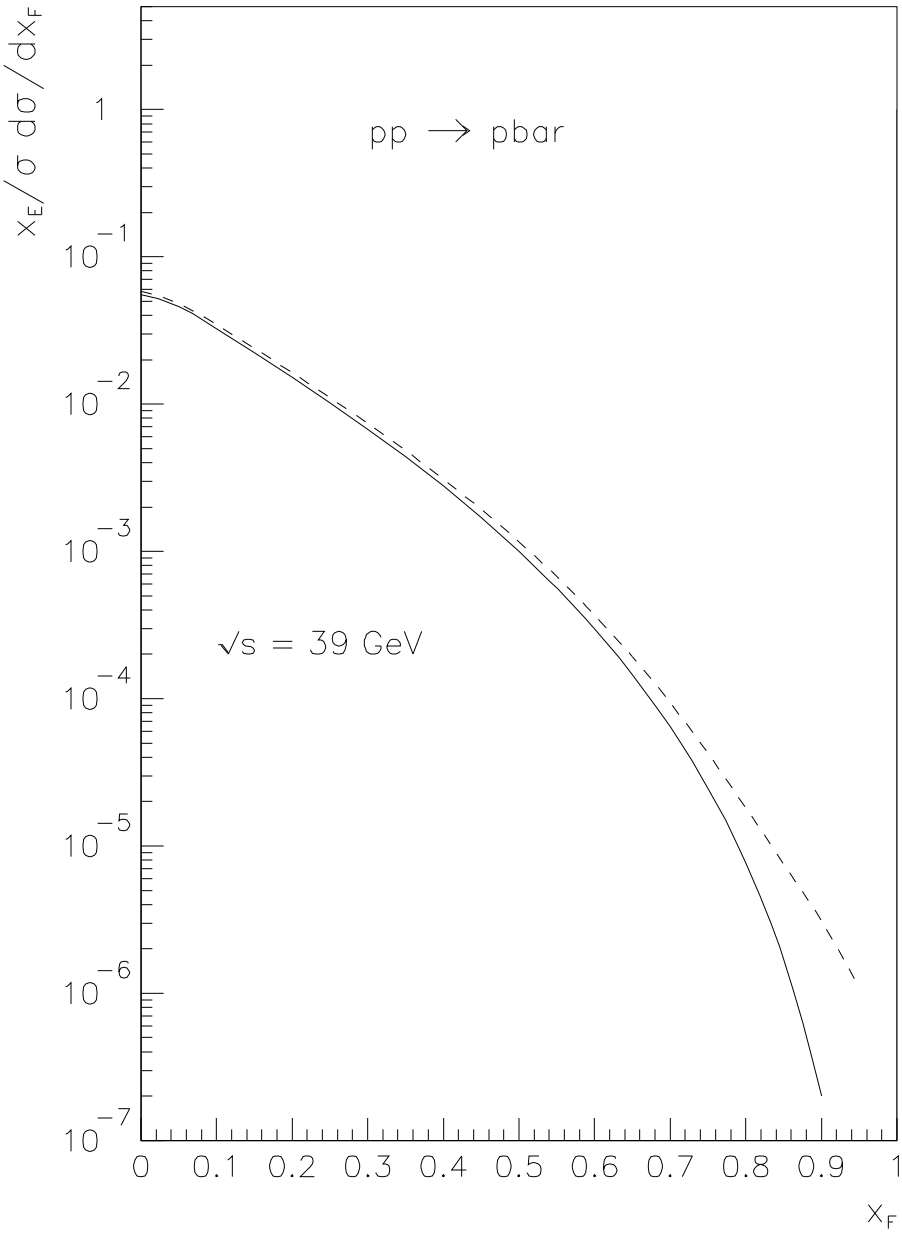

$x_E/\sigma\ d\sigma/dx_F$
pp → pbar
√s = 39 GeV
1
$10^{-1}$
$10^{-2}$
$10^{-3}$
$10^{-4}$
$10^{-5}$
$10^{-6}$
$10^{-7}$
0
0.1
0.2
0.3
0.4
0.5
0.6
0.7
0.8
0.9
1
$x_F$

Fig. 3a

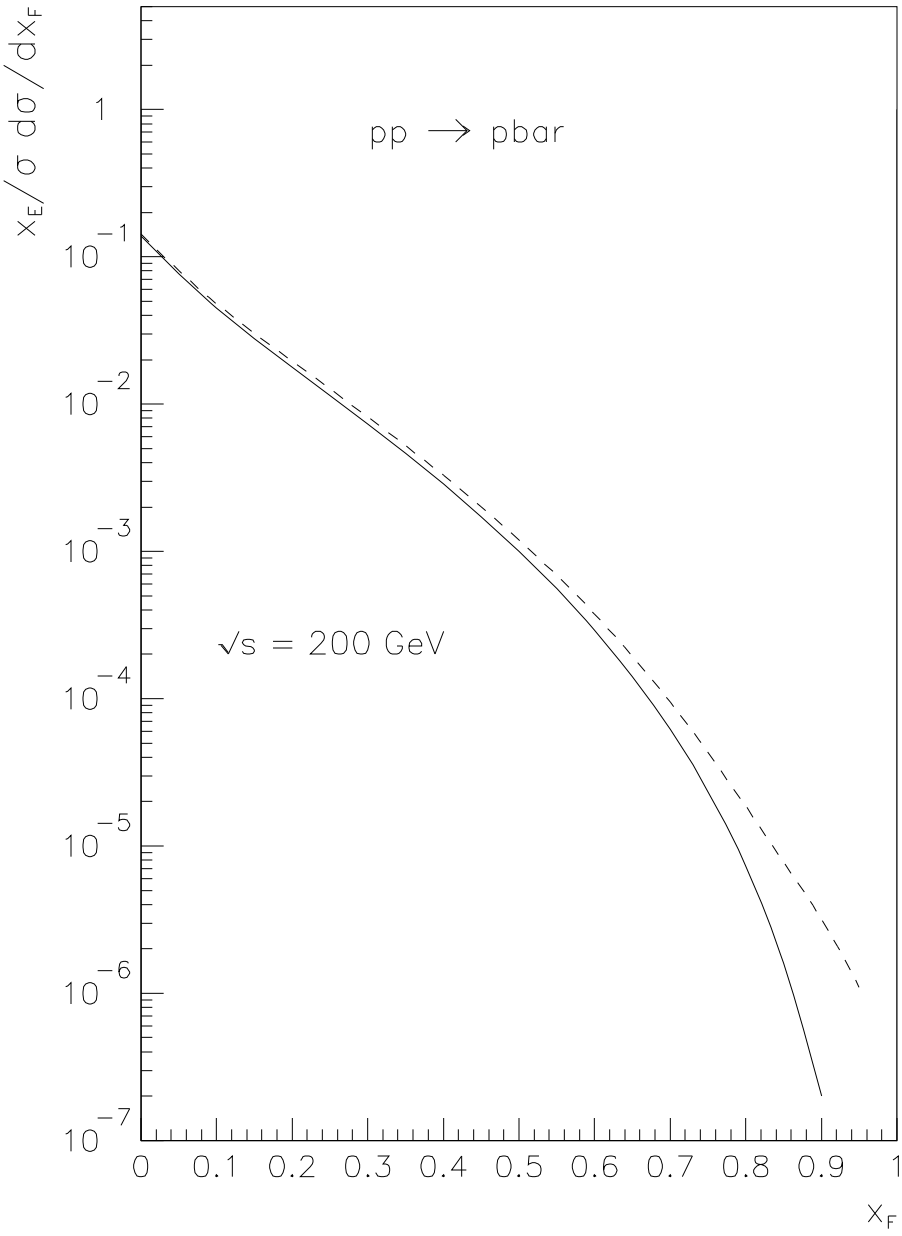

$x_E/\sigma\ d\sigma/dx_F$
1
$10^{-1}$
$10^{-2}$
$10^{-3}$
$10^{-4}$
$10^{-5}$
$10^{-6}$
$10^{-7}$
pp $\rightarrow$ pbar
$\sqrt{s}$ = 200 GeV
0
0.1
0.2
0.3
0.4
0.5
0.6
0.7
0.8
0.9
1
$x_F$

Fig. 3b

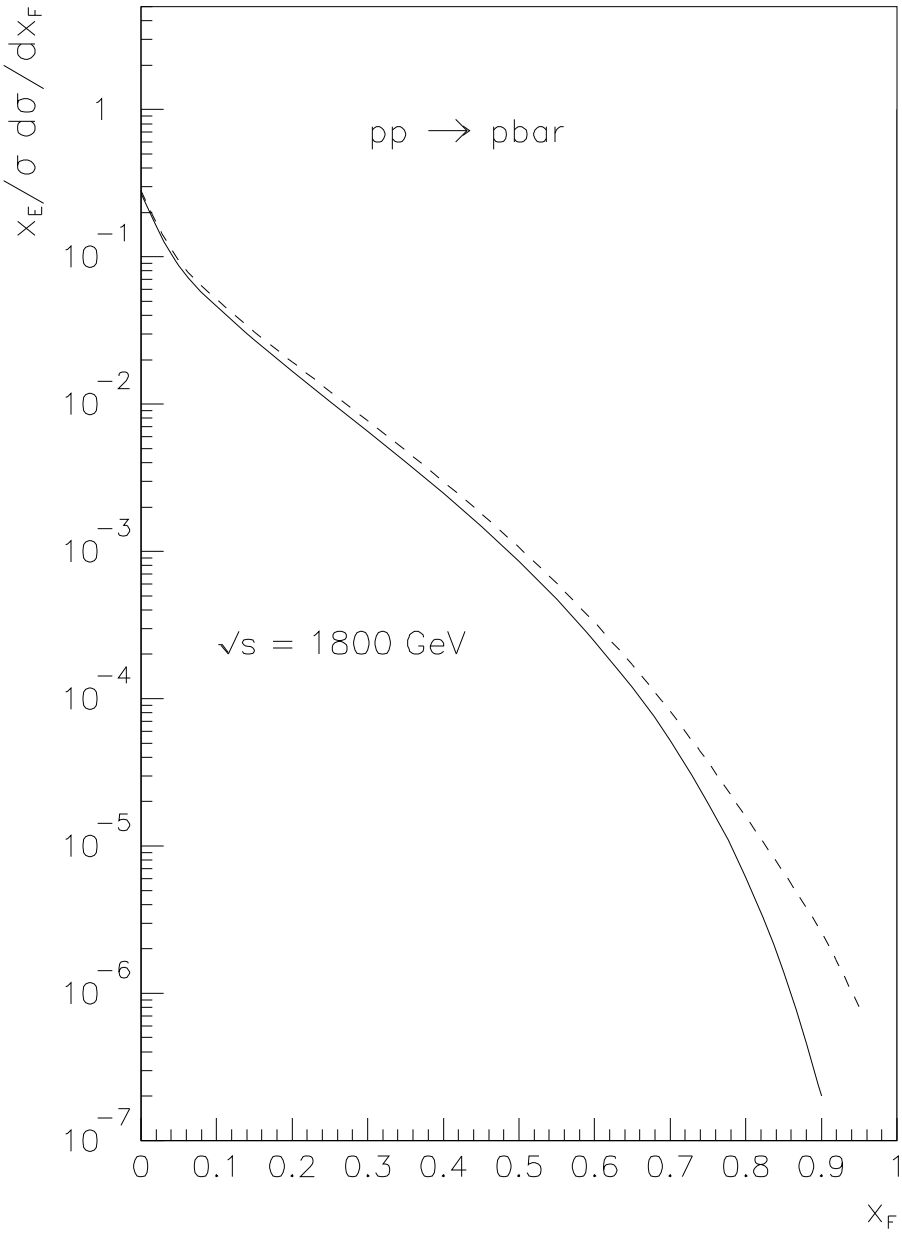

$x_E/\sigma\ d\sigma/dx_F$
pp → pbar
√s = 1800 GeV
1
$10^{-1}$
$10^{-2}$
$10^{-3}$
$10^{-4}$
$10^{-5}$
$10^{-6}$
$10^{-7}$
0
0.1
0.2
0.3
0.4
0.5
0.6
0.7
0.8
0.9
1
$x_F$

Fig. 3c

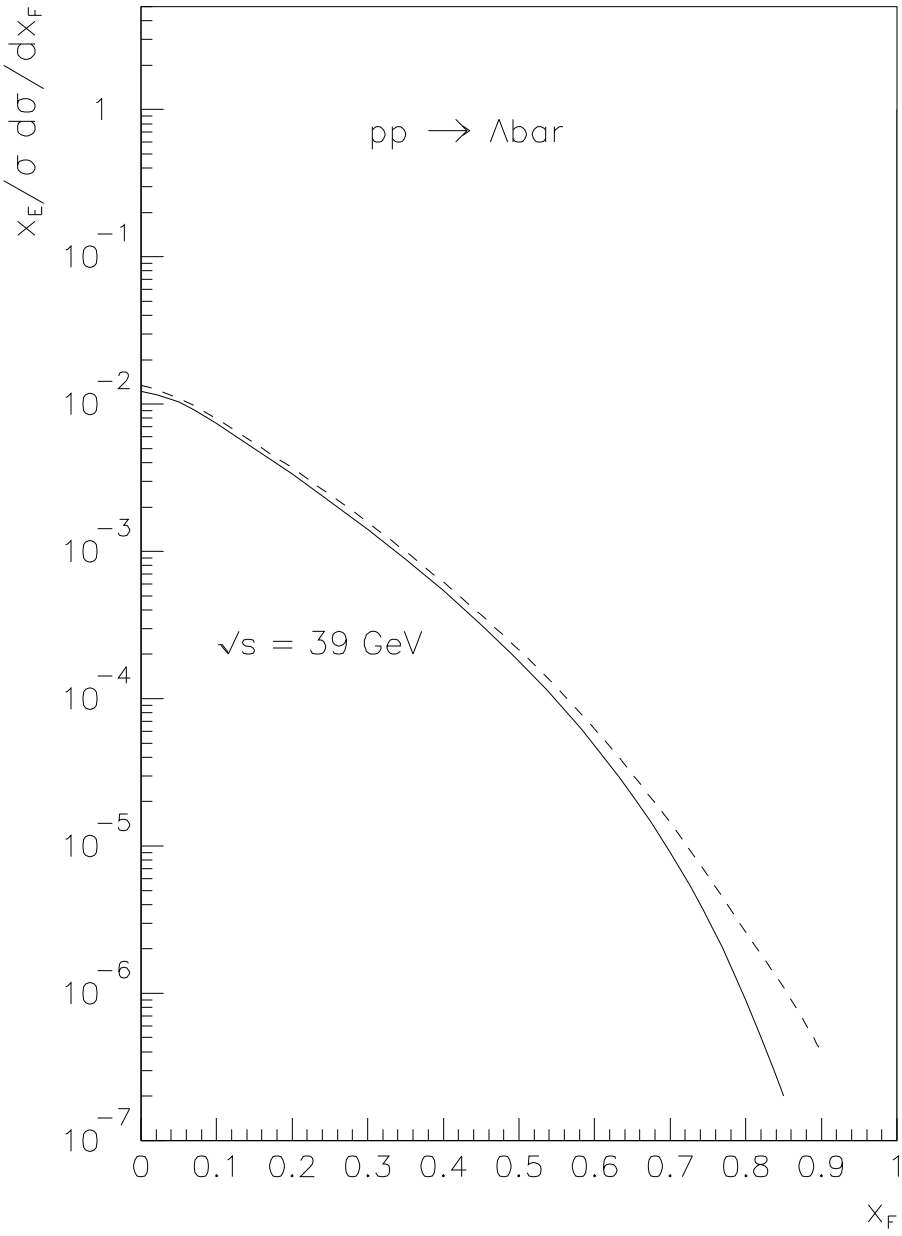

$x_E/\sigma\ d\sigma/dx_F$
pp → Λbar
√s = 39 GeV
1
$10^{-1}$
$10^{-2}$
$10^{-3}$
$10^{-4}$
$10^{-5}$
$10^{-6}$
$10^{-7}$
0
0.1
0.2
0.3
0.4
0.5
0.6
0.7
0.8
0.9
1
$x_F$

Fig. 4a

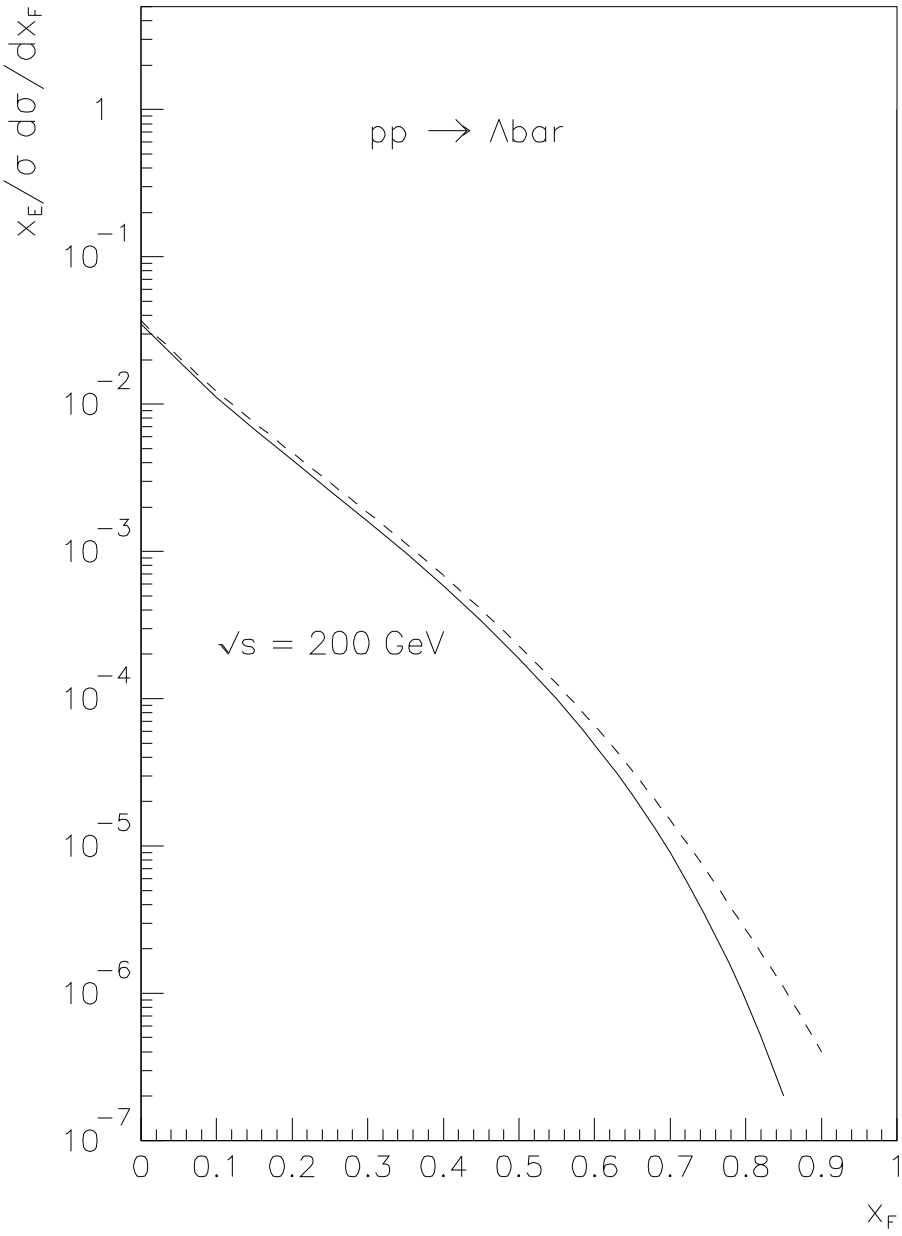

$x_E/\sigma\ d\sigma/dx_F$
pp $\rightarrow$ Λbar
√s = 200 GeV
1
$10^{-1}$
$10^{-2}$
$10^{-3}$
$10^{-4}$
$10^{-5}$
$10^{-6}$
$10^{-7}$
0
0.1
0.2
0.3
0.4
0.5
0.6
0.7
0.8
0.9
1
$x_F$

Fig. 4b

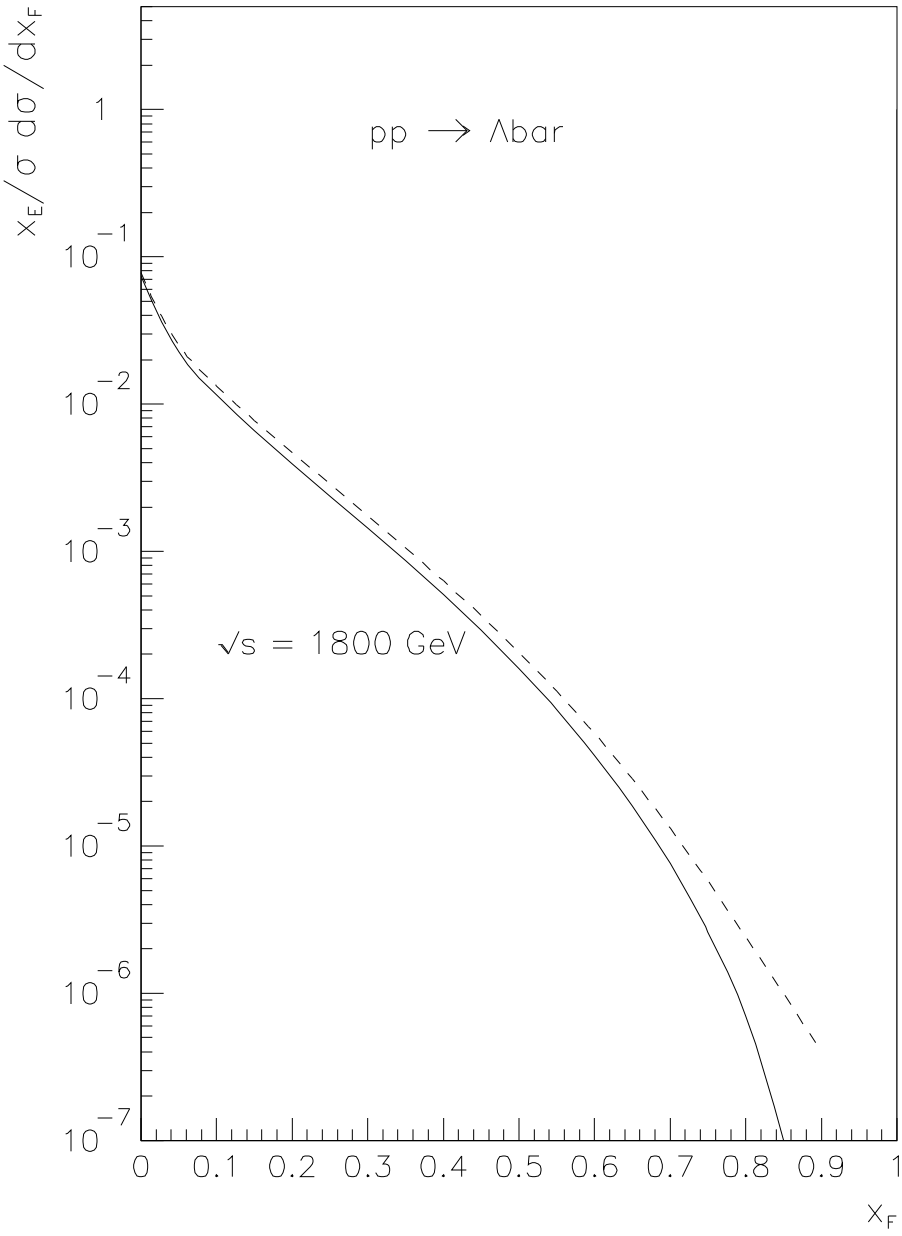

$x_E/\sigma\ d\sigma/dx_F$
pp → Λbar
√s = 1800 GeV
1
$10^{-1}$
$10^{-2}$
$10^{-3}$
$10^{-4}$
$10^{-5}$
$10^{-6}$
$10^{-7}$
0
0.1
0.2
0.3
0.4
0.5
0.6
0.7
0.8
0.9
1
$x_F$

Fig. 4c

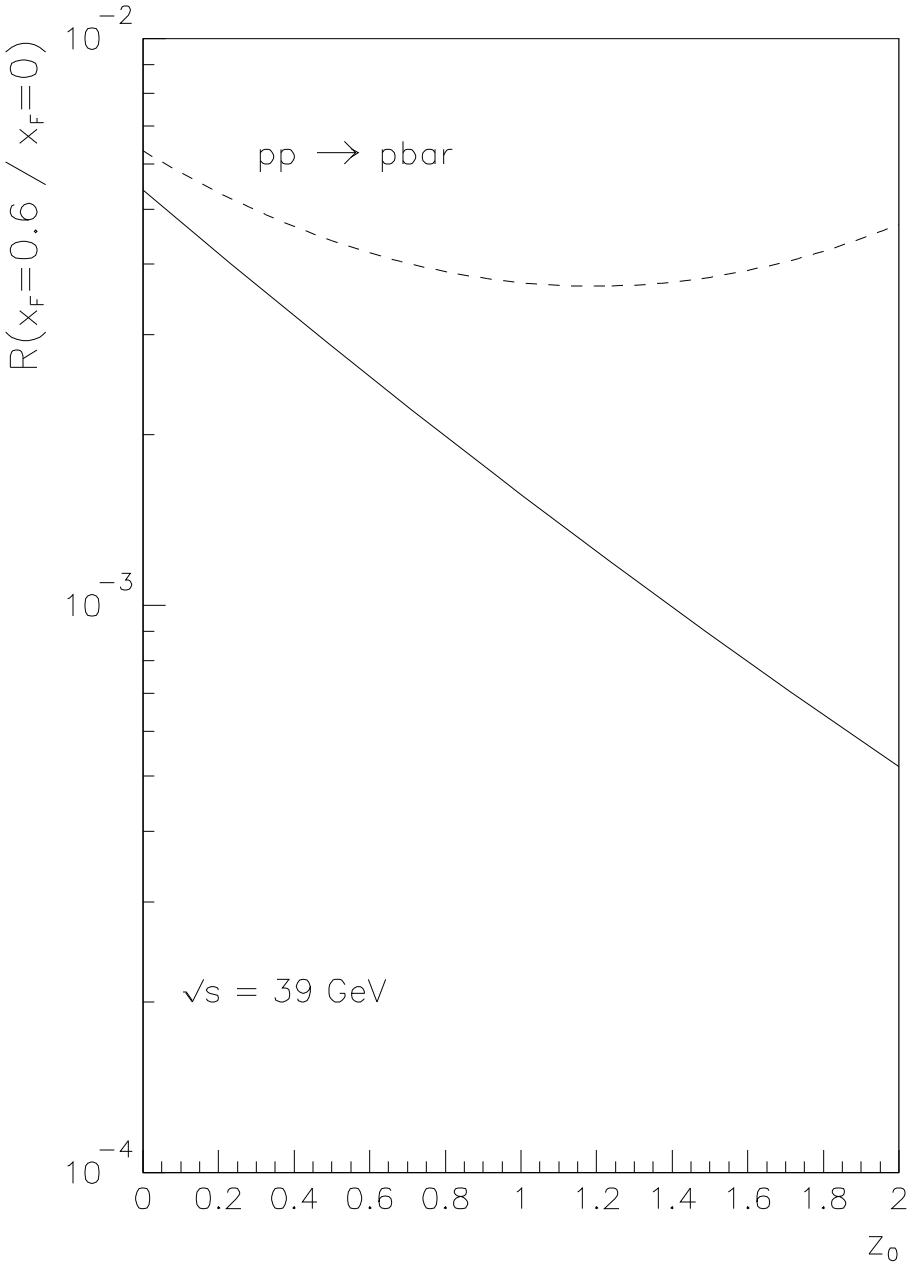

$10^{-2}$
$10^{-3}$
$10^{-4}$
$R(x_F=0.6\ /\ x_F=0)$
pp $\rightarrow$ pbar
$\sqrt{s}$ = 39 GeV
0
0.2
0.4
0.6
0.8
1
1.2
1.4
1.6
1.8
2
$z_0$

Fig. 5a

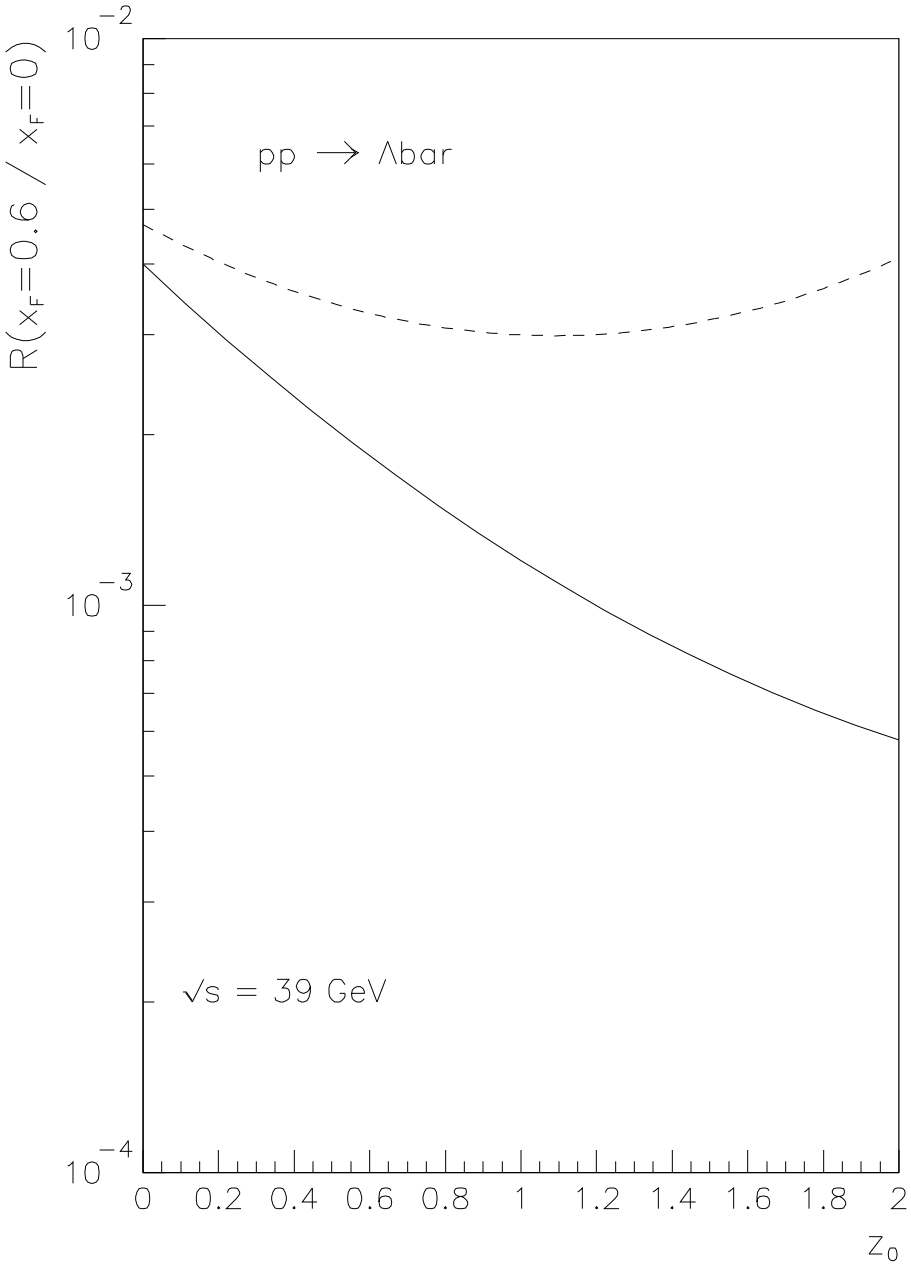

$10^{-2}$
$10^{-3}$
$10^{-4}$
$R(x_F=0.6\ /\ x_F=0)$
pp $\rightarrow$ Abar
$\sqrt{s}$ = 39 GeV
0
0.2
0.4
0.6
0.8
1
1.2
1.4
1.6
1.8
2
$z_0$

Fig. 5b